Naval Information Warfare Center PACIFIC

TECHNICAL DOCUMENT 3409
SEPTEMBER 2021

Method Development for Magnetometer Coils Using Additive Manufacturing

Kathryn M. Liotta
Eric Bozeman
Angelica V. Sarmiento
Lewis Hsu
Yolanda Meriah Arias-Thode

NIWC Pacific

Naval Information Warfare Center Pacific (NIWC Pacific)
San Diego, CA 92152-5001

This page is intentionally blank.

TECHNICAL DOCUMENT 3409
SEPTEMBER 2021

Method Development for Magnetometer Coils Using Additive Manufacturing

Kathryn M. Liotta
Eric Bozeman
Angelica V. Sarmiento
Lewis Hsu
Yolanda Meriah Arias-Thode

NIWC Pacific

Administrative Notes:
This Document was approved through the Release of Scientific and Technical Information (RSTI) process in December 2020 and formally published in the Defense Technical Information Center (DTIC) in September 2021.

NIWC Pacific
San Diego, CA 92152-5001

NIWC Pacific
San Diego, California 92152-5001

A. D. Gainer, CAPT, USN
Commanding Officer

W. R. Bonwit
Executive Director

ADMINISTRATIVE INFORMATION

The work described in this report was performed by the Basic & Applied Research Division of the Cyber, Science & Technology Department, Naval Information Warfare Center Pacific (NIWC Pacific), San Diego, CA. The NIWC Pacific Naval Innovative Science and Engineering (NISE) Program provided funding for this Basic Applied Research project. Further assistance was provided by the Naval Acquisition Career Center (NACC), as well as the Office of Naval Research (ONR), Grant number: N0001420WX00313.

Released by
John deGrassie, Division Head
Basic & Applied Research Division

Under authority of
Carly Jackson, Department Head
Cyber, Science & Technology Department

ACKNOWLEDGMENTS

We would like to acknowledge Teresa Emery, of NIWC Pacific for her awesome technical assistance in use of the 3D printer.

Editor: MRM

EXECUTIVE SUMMARY

This report presents the methods and results of a short study with the goal of producing fluxgate magnetometer sensors with a higher sensitivity and lower power requirements than the first generation designed by the Non-Linear Dynamics group at Naval Information Warfare Center (NIWC) Pacific. To achieve this goal, additive manufacturing technology was evaluated as a means to increase sensitivity and decrease power requirements. The windings of the magnetometer sensor should have a smaller diameter and be closer to the core material to decrease the air gap to increase sensitivity in the pick-up coil, and reduce power requirements for the excitation coil. Most methods presented in this report focus on the use of the Optomec aerosol jet printer, and outlined are the challenges of each method. A more likely approach to solve these issues is also presented; and this is the use of actual wires for the windings instead of depending on the additive manufactured conductive lines.

This page is intentionally blank.

ACRONYMS

BMFC	Benthic Microbial Fuel Cell
CAD	Computer Aided Design
UV	Ultraviolet

This page is intentionally blank.

CONTENTS

FIGURES

TABLES

1. INTRODUCTION

In this study, various approaches are explored to develop a magnetometer sensor that requires less power and is more sensitive than existing devices. A previous study constructed a magnetometer that required 100 mW of power (Arias-Thode, et al., 2017) [1]. In that study, benthic microbial fuel cells (BMFC) charged a battery to support a magnetometer for about 38 days. If a magnetometer coil is developed that uses less power, then the magnetometer device will last longer when powered by the BMFC system. This study focuses on developing the coil part of the magnetometer, which is illustrated Figure 1.

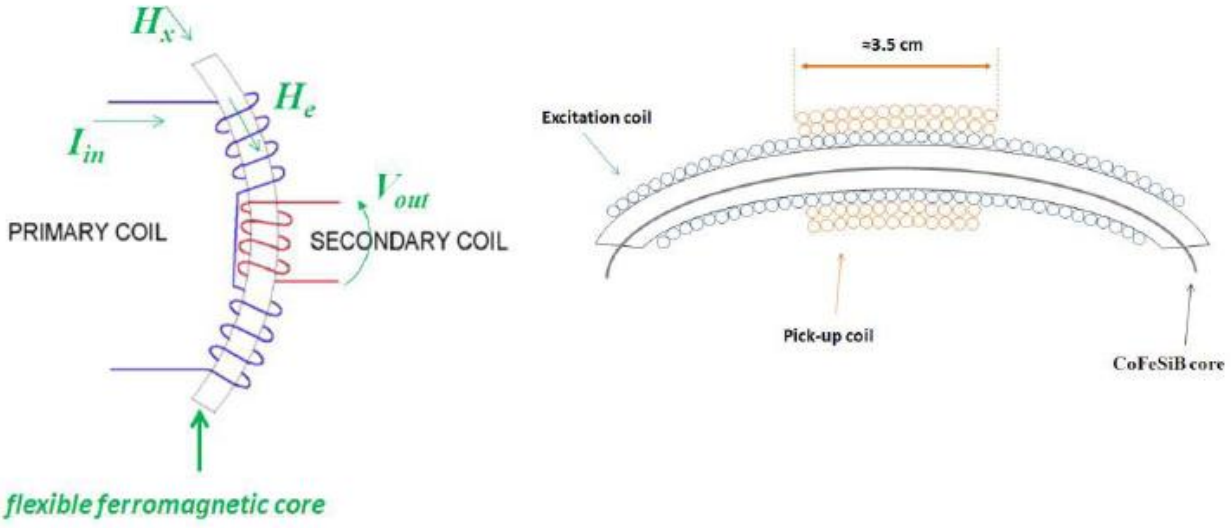

Figure 1. Schematic and cross-section of the magnetometer device. Figure is from reference (Trigona, Sinatra, Andò, Baglio, & Bulsara, 2017) [5].

In order to improve the sensitivity, the diameter of the magnetometer's excitation and pick-up coils are made as small as possible. Previous coils were made around a rigid plastic support, which caused the coils to have larger diameters with the ferromagnetic core suspended inside. Removing the plastic support allows the coil to wrap around the core more closely. Because of the small size desired, most of the approaches in this study utilize an Aerosol Jet® AJ 200 System, manufactured by Optomec. Aerosol jet printing is like "tiny spray painting." In this study, silver ink is used to print wires. The process aerosolizes ink and then focuses it to a final output diameter of 20-60μm. Benefits of aerosol jet printing are small feature size and ability to print on a wide variety of materials and terrains (roughness up to a couple millimeters). This study explores four approaches for creating magnetometer coils.

1.1 APPROACH #1: "SANDWICH" METHOD

The CoFeSiB core for the magnetometer has a wire-like shape with a diameter of about 100μm. The core material is specially annealed to align its magnetic domains, and exposure to stress or strain may result in decreased effectiveness. The silver ink (and nearly all conductive inks) must be cured after printing in order to reach maximum conductivity. Traditional curing methods introduce heat that would cause damage. For this reason, the approach attempted in this study is: print two complementary patterns that can be "sandwiched" together with the core material in between to

create a complete circuit around the core. Figure 2 shows the preliminary design, which includes 4.5 turns of the coil.

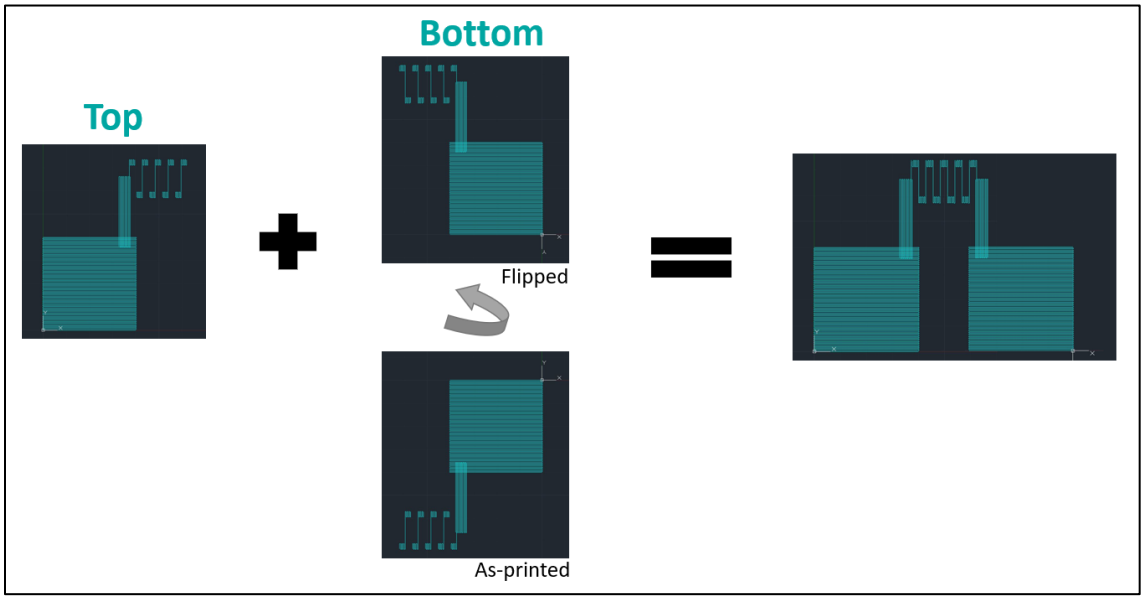

Figure 2. CAD for complementary patterns to create a coil.

Dimensions for the preliminary design are selected as shown Figure 3. These dimensions were selected because they seemed obtainable and insightful for feasibility of a more complex design.

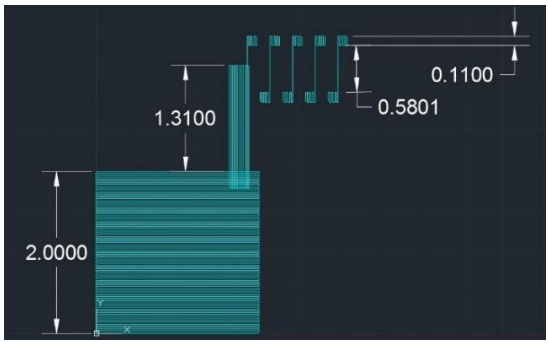

Figure 3. Dimensions (in mm) for coil design.

The design was printed onto glass slides and plastic sheets. The printing parameters are listed in Table 1. The resulting line width was 30μm. A microscope image of one of the printed designs is shown in Figure 4.

Table 1. Aerosol jet printing parameters.

Parameter	Value
Nozzle opening diameter	200µm
Ink	Silver Ink: HPS-108AE1
Sheath Flow	70 sccm
Exhaust Flow	640 sccm
Atomizer Flow	650 sccm
Stage Speed	3 mm/sec

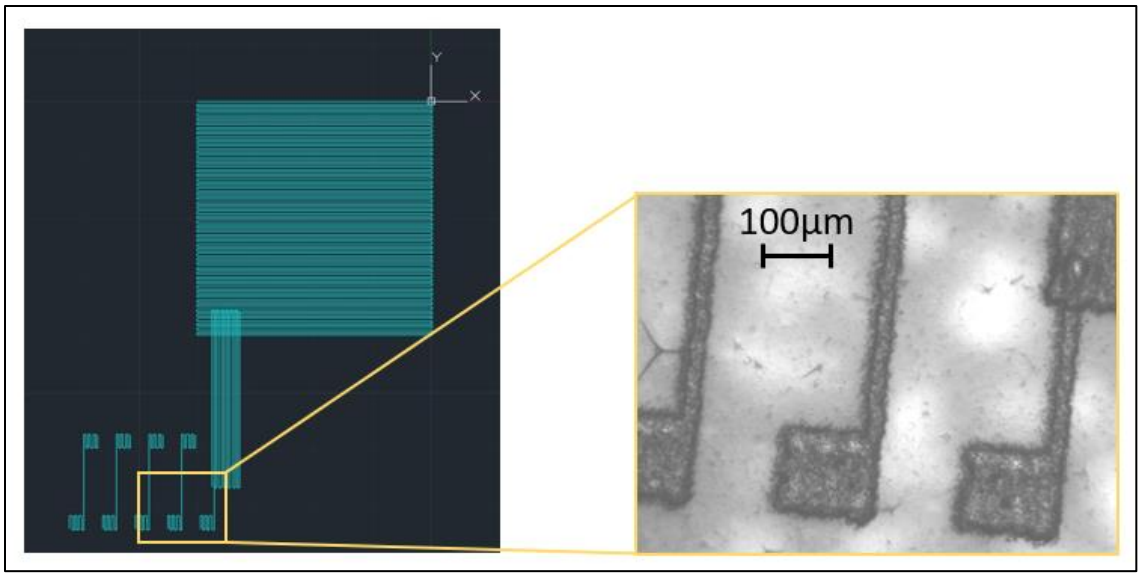

Figure 4. Schematic to show microscope image of printed design on a plastic sheet.

All the prints were cured in the Xenon X-1100 High-Intensity Pulsed Light System with a power of 2kV, with a time of 2ms, and with the sample placed on the 8th shelf (one above the bottom shelf). Next, an attempt was made to use Norland Optical Adhesive (UV curing) to stick a top and bottom of the design on plastic together. Ten minutes of UV exposure cures the optical adhesive. The designs were aligned by eye (this was just barely possible) and then checked using the microscope. As shown in Figure 5, the upper contact points of the coil are aligned very well. The lower contact points are not aligned as well, but made the desired contacts.

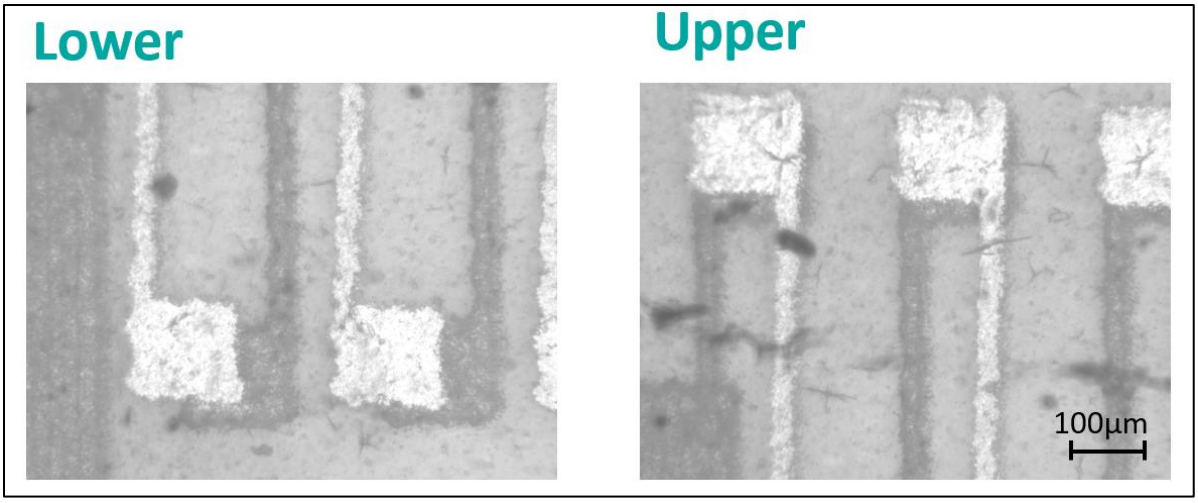

Figure 5. Alignment of upper and lower coil contacts.

Because the device is so small, it is difficult to capture in a photograph, but an attempt is shown in Figure 6. The glass slide was used as support for moving the sample around before the adhesive is cured. Some adhesive is visible as brighter spots, as labelled in Figure 6. When assembled, the contact pads of each piece were inside the "sandwich". The plastic was trimmed back so the pads were exposed to the exterior of the device; one facing upwards, and the other facing down. To allow access to both contact pads from the same side of the device, aluminum foil (resistance <1 Ω, not present in Figure 6) was attached to the downward facing pad. The foil extended beyond the plastic so that probe tips could connect to each pad on the same side of the device. The device "sandwich", along with the foil, were pressed together using fingers or a binder clip with thin cardboard on both sides. The resistance through the device varied depending on the pressure being applied to hold the device together. When the experimenter applied enough pressure to close the circuit (connecting the coil contacts, as shown aligned in Figure 5), the typical resistance values were in the range of 30-60Ω. The binder clip was also successful at holding the sides together, which led to lower resistances of 5-15Ω.

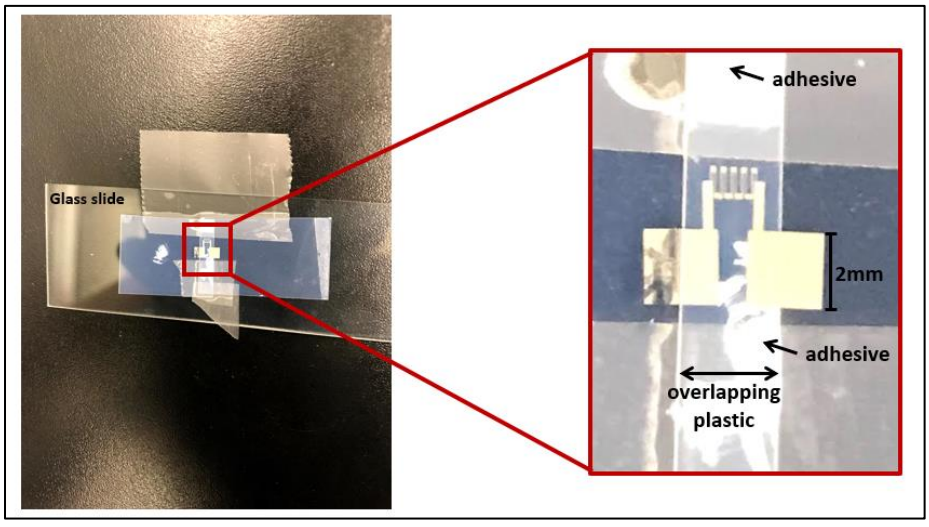

Figure 6. Image of complete coil device, with top and bottom printed on plastic.

1.2 APPROACH #2: ALIGNMENT METHOD

A new method was implemented because the previous method required maintaining active pressure to hold the pieces together. This new method involves printing the bottom part of the coil with alignment marks, securing the core using an adhesive, and then realigning the coil+core in the printer to print the top part of the coil. This process is displayed in Figure 7.

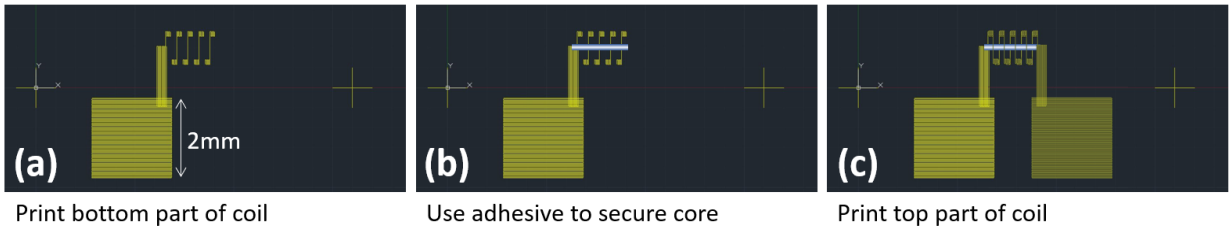

Figure 7. Schematic of the new fabrication method using CAD images for (a) printing the bottom part of the coil, (b) applying the adhesive and core, and (c) printing the top part of the coil.

In order to understand the effectiveness of each step of the process, the following coils, representing each step were prepared and evaluated:

1. Bottom and top printed on day 1
2. Bottom printed on day 1 and top printed on day 2
3. Bottom and top printed on day 2
4. Bottom printed on day 1 with adhesive applied in core region and top printed on day 2
5. Bottom printed on day 1 with adhesive and core applied and top printed on day 2

The resistance (from 2 different multimeters: Fluke 27 and Amprobe) and inductance measurements are displayed in Table 2. All of these coils are printed on glass because the UV curing adhesive does not allow for enough precision on the mesoporous plastic. The glass substrate probably caused some of the increase in resistance compared to the plastic used in the previous approach. This might be because the pulsed light system was optimized to cure silver ink on the plastic, but not glass. It is possible that the light curing could be optimized better for curing the silver ink on glass.

Table 2. Resistances and inductances of each variation of coil using the new fabrication method.

Coil	Resistance (Fluke 27)	Resistance (Amprobe)	Inductance (Amprobe)
1) Both sides printed 7/6	131 Ω	123 Ω	0.135 mH
2) Bottom 7/6, Top 7/13	567 Ω	570 Ω	1.43 mH
3) Both sides printed 7/13	8.34 kΩ	8.35 kΩ	0.8 mH
4) With UV curing adhesive	267 kΩ	8.81 kΩ	0.88 mH
5) With adhesive and core	-	-	-

Comparison of coils 1 and 3 in Table 2 show that the print quality was much better (lower resistance) on the first printing day compared to the second printing day. The difference in quality was due to the ink's settling and evaporation of solvents over time, causing an increase in the ink's viscosity and a decrease in its printing performance. It is unclear why one multimeter displayed a

larger increase in resistance from adding the adhesive between core layers, but the other multimeter displayed a smaller increase (compare coils 2 and 4 in Table 2).

Inductance (L) is calculated using Equation 1, where μ is the permeability of the core material, N is the number of turns of the coil, A is the cross-sectional area of the coil, and l is the length of the coil.

$$L = \frac{\mu N^2 A}{l} \qquad \text{Equation 1}$$

When both sides of the coil are printed onto the same surface with nothing in the core region (such as coils 1-3 in Table 2), the inductance is expected to be zero because the cross-sectional area is zero. When something (adhesive or adhesive+core) is added to the core region of the coil, the inductance is expected to increase due to the increase in cross-sectional area. The inductance data in Table 2 does not display this trend. However, when using the multimeter to measure the inductance, the results were inconsistent (failed to hold a steady measurement), so the displayed valued might be unreliable. It was possible that the multimeter measurement picked up inductances from the probes, pads, and other parasitic inductances. Unfortunately, in this series of coils, coil 5 (with the core) resulted in an open circuit. Images of coils 4 and 5 are shown in Figure 8.

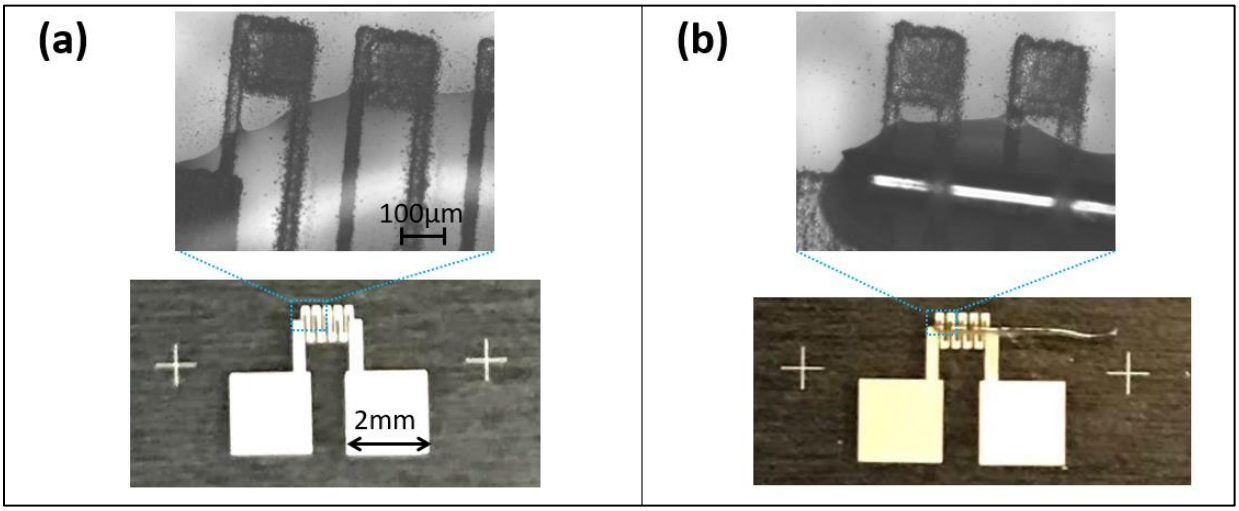

Figure 8. Macroscopic and microscopic images of final devices: (a) coil 4 and (b) coil 5 from Table 2.

The following options were considered to insulate the core material: liquid electrical tape, pipe thread sealant, Superior Weather Seal, 3M Hi-Strength 94ET Spray Adhesive, Loctite Spray Adhesive, and nail polish. Of those, only the liquid electrical tape and nail polish provided successful coatings. The nail polish is a little easier to handle than the liquid electrical tape because it is thinner and has a more precise brush.

For the next batch of prints, two pieces of core material were coated with nail polish to provide an insulative layer between the core and the coil. Then, the cores were secured to the devices using UV curing adhesive and the top parts of the coils were printed. Unfortunately, neither of these devices make a complete circuit. The images in Figure 9 provide some evidence for why the devices do not conduct. In Figure 9a (coil 1), there appears to be a bubble in the UV curing adhesive that was used to bind the core to the coil, which may have caused a break in the printed wire. In Figure 9b (coil 2), there was a discontinuity in each wire that was printed on top of the core. For coil 1, two layers of the top part of the coil were printed. For coil 2, four layers of the top part of the coil were printed. It is possible that printing additional layers of the coil will complete the circuit. It is also important to note

that none of the ink for these coils was cured in the oven or light box, which might also contribute to the inability to measure a resistance. While uncured silver ink is typically conductive, it has a higher resistance. However, in this case the curing step was skipped because it did not improve the conductivity of wires printed on glass and an oven would change the magnetic properties of the core.

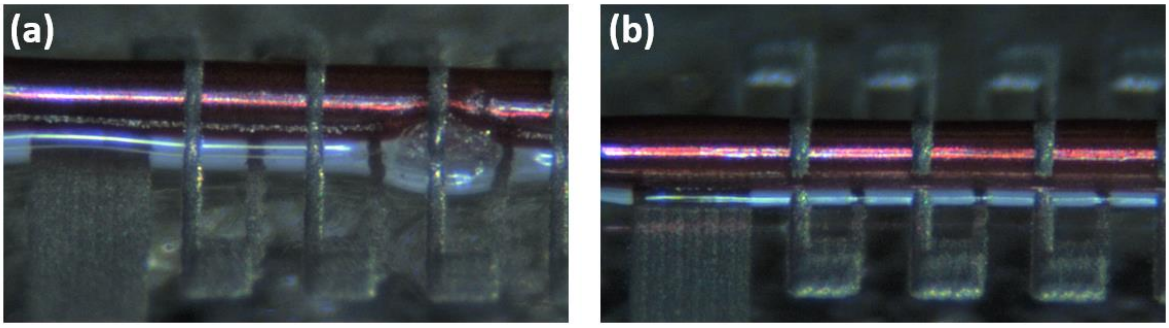

Figure 9. Process camera images of (a) coil 1 and (b) coil 2 with nail polish coated cores.

1.3 APPROACH #3: SERVO METHOD

The next approach is the servo method. In this method, a 360° servo is used to print a coil around piece of insulation removed from a 30-gauge wire, so the core can be inserted inside afterward. The CAD drawing for this method is displayed in Figure 10. First, the contact pads and alignment are printed when the insulation is stationary. Then, the line is printed while the wire plastic is rotating, creating a coil.

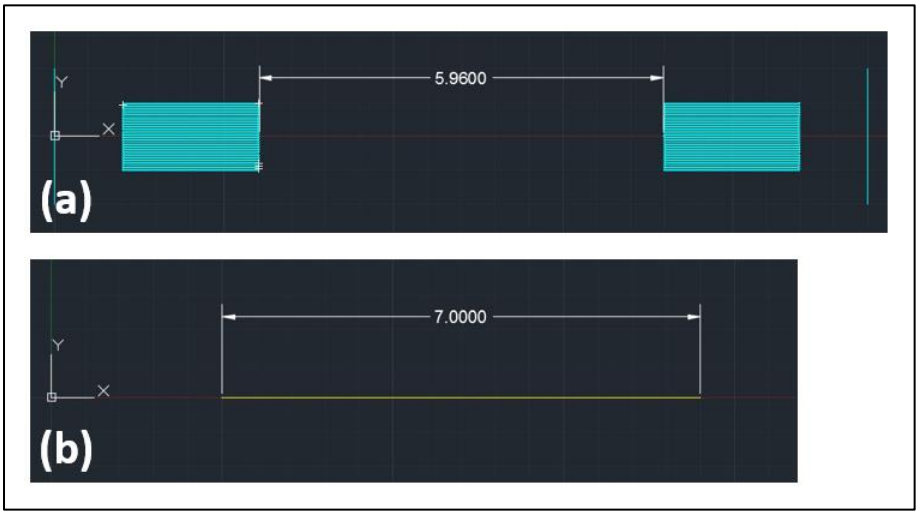

Figure 10. CAD for printing (a) contact pads and alignment marks, and then (b) the coil onto plastic from stripped wire.

First, to check the wire plastic compatibility with the printed ink, the pattern was printed onto a stationary wire plastic, as shown in Figure 11. After printing, none of the prints conducted. However, after light curing (Xenon X-1100, 2kV, 2ms, 8th shelf) three of the four prints conducted. The resulting resistances are shown in Table 3. Each consecutive (single layer) print was aligned better on top of the cylindrical plastic. This resulted in four separate prints along the plastic. The wide range of resistances indicates that it will be challenging to align and print while rotating the wire plastic. If aligning and printing the coil is successful, treating the wire plastic with oxygen plasma could possibly help the ink adhere better.

Figure 11. Contact pads with a single trace connecting them, printed on wire plastic casing.

Table 3. Resistances of patterns printed onto stationary wire plastic.

Print	Resistance
1	-
2	13.5 MΩ
3	7 MΩ
4	500 Ω

In order to print onto the wire plastic while it is spinning, the printing speed of the stage needs to be coordinated with the rotation of the servo. The first step was to figure out what pulse input would be required to cause the servo to rotate at particular speeds. The pulse lengths produced by the programmed board were confirmed using an oscilloscope. The experimental results of the resulting servo rotation from various programmed pulse lengths are shown in Figure 12. The speeds as a result of certain input pulse lengths were not consistent. For example, a pulse length of 1.6 ms resulted in rotation speeds of 12, 26, and 42 rpm. Sometimes, restarting the device causes a drastic change in speed, even though the pulse is unchanged. A stepper motor would provide more reliable speeds.

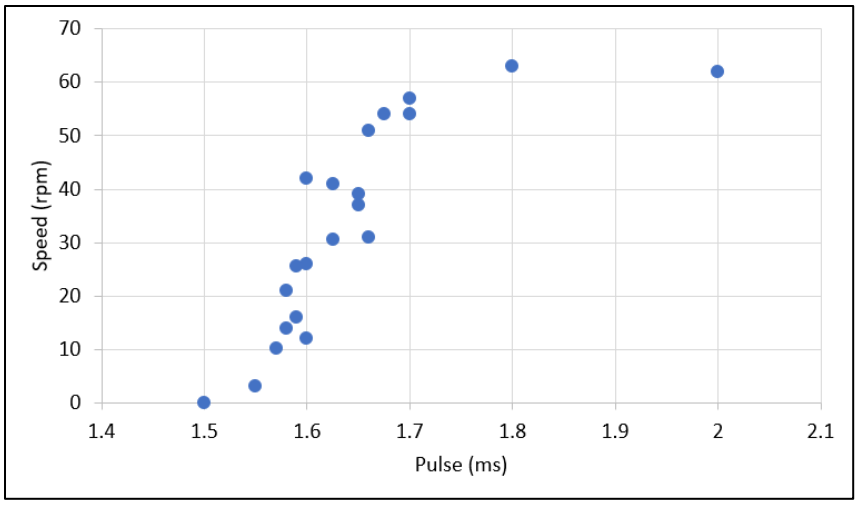

Figure 12. The effect of pulse coded onto the servo on rotation speed.

The horizontal speed of the stage (from printing the line) versus the rotation speed was calculated for effective print speeds of 1-5 mm/sec, which is the typical printing range. The resulting values are shown in Table 4. The wire plastic's diameter was assumed to be 1 mm and the distance between coil windings (assuming zero width) was assumed to be 0.1 mm, or 100 μm.

Table 4. Horizontal and rotational speeds calculated to achieve various effective speeds.

Effective Speed (mm/sec)	Horizontal Speed (mm/sec)	Rotational Speed (rpm)
1	0.03	19
2	0.06	38
3	0.10	57
4	0.13	76
5	0.16	95

The stage is able to print at all the horizontal speeds listed in Table 4, but the servo can only achieve rotational speeds up to 63 rpm. The desired effective speed varies each day and depends on factors such as the ink viscosity and cleanliness of the printing nozzle. If a lot of ink is coming out of the nozzle, then a higher effective speed is necessary to avoid excessive buildup and splattering of the ink. A way to minimize splattering is by heating the substrate, but because the substrate will be attached to the servo, heating it is not possible.

This method was not carried out due to time and material constraints. An anticipated challenge would be maintaining a continuous print on the plastic while it is spinning because the plastic is not perfectly straight.

1.4 APPROACH #4: WIRE METHOD (NO PRINTING)

None of the previous methods were successful for completing a coil with the core incorporated. A magnetometer sensor of a similar size scale to the previous methods was constructed using a fine wire (~100 μm) coated in nail polish to insulate it. The coils were wrapped around blue insulation (outer diameter ~480 μm) that was stripped from a wire. These hand-wound coils are shown in Figure 13 and Figure 14.

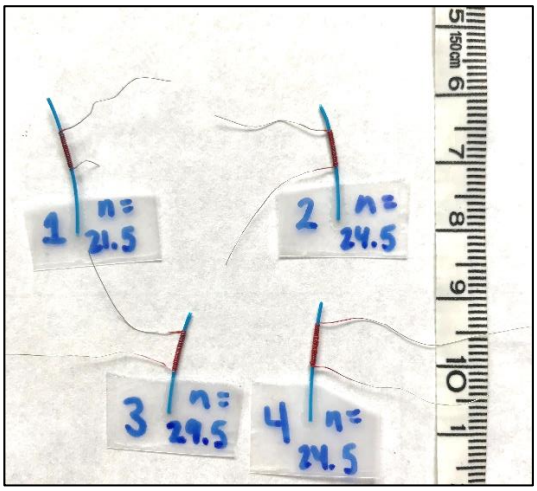

Figure 13. Four hand-wound coils with labeled number of turns.

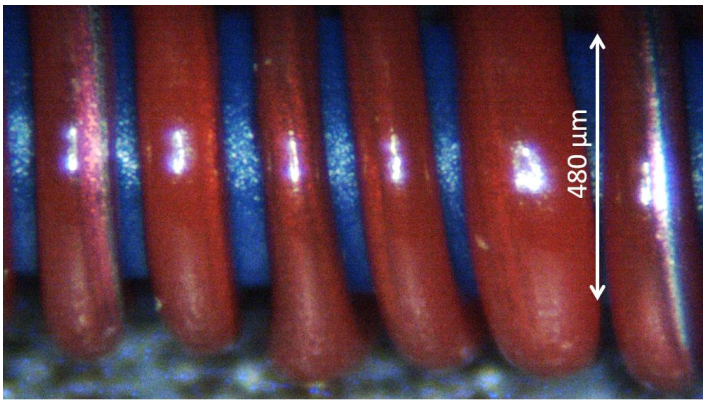

Figure 14. Microscope image of hand-wound coil #2 from Figure 13.

The resistance, as well as the measured and calculated inductances for these coils with and without the core material are listed in Table 5. The Amprobe multimeter was used for the resistance and inductance measurements. The values for inductance were calculated using Equation 1. For the calculation, the permeability of the plastic and nail polish were assumed to be negligible. The relative permeability of the core material was assumed to be 80000 (Trigona, Sinatra, Andò, Baglio, & Bulsara, 2017) [5]. When the core was inserted, the measured inductance increased by about 100% because of the increased permeability. The device with the core was probably far from the theoretical inductance value because the material was damaged due to handling or temperature, greatly reducing its relative permeability.

Table 5. Resistances and inductances of the hand-wound coils (with and without core).

Coil Number	Measured Resistance (Ω)	Measured Inductance without core (µH)	Calculated Inductance without core (µH)	Measured Inductance with core (µH)	Calculated Inductance with core (µH)
1	0.08	3.8	0.028	6.0	2200
2	0.13	6.0	0.033	12	2600
3	0.12	4.6	0.043	9.8	3500
4	0.14	4.9	0.029	8.2	2300

There are about two orders of magnitude between the measured and calculated inductance in Table 5. However, the inductance measurements were suspected to be unreliable when measuring the devices from approach #2 because in that case, the inductance was calculated to be zero. The measured inductances of the approach #2 devices were actually much higher (measured values of about 1 mH) even though they were expected to be smaller due to the geometries of the devices.

The size comparisons for all the methods are shown in Table 6. The coil diameters listed for the first three approaches are the largest cross-sectional dimensions because the design is mostly 2D. The distance between coil windings is mostly due to the thickness of insulation on coil wires for approach #4. The dimensions for the first three approaches are limited by the need to hand-assemble the devices.

Table 6: Dimensions attempted in approaches 1-3 compared to theoretical dimensions possible for approach #4.

	Approach #1 (unsuccessful)	Approach #2 (unsuccessful)	Approach #3 (theoretical)	Approach #4 (achieved)	Approach #4 (theoretical)
Wire diameter	30-50 µm	30-50 µm	30-50 µm	100 µm	51 µm
Coil diameter	580 µm	580 µm	≤480 µm	550 µm	≥150 µm
Distance between coil windings	~100 µm	~100 µm	~100 µm	~130 µm	≥5 µm

The magnetic field (B) produced by an empty coil is calculated using Equation 2, where μ_0 is the permeability of free space, n is number of coil turns, a is radius of the coil, I is current, and z is the axial distance from the center of the coil.

$$B = \frac{\mu_0 n a^2 I}{2(a^2 + z^2)^{3/2}} \qquad \text{Equation 2}$$

When constant values are assumed for all parameters except for current and coil radius, the resulting relationship is shown in Figure 15. This curve shows that when the coil is used to create a magnetic field, the amount of current that it takes to create a certain magnetic field strength at a particular distance away, increases exponentially as the coil radius decreases. This means that when the coil is used to pick-up a magnetic field, sensors with a smaller radius will be more sensitive.

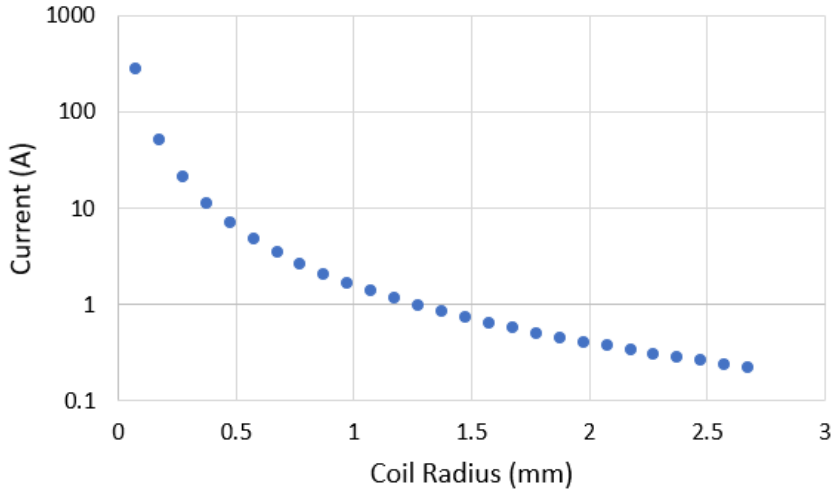

Figure 15. The effect of coil radius on current calculated from Equation 2 when all other parameters remain constant.

The coil could be made even smaller using Approach #4, as shown in the last two columns of Table 6. In order to achieve the dimensions listed in the theoretical column, the procedure assumes the use of an automatic coil winding machine, 44 AWG magnet wire (Magnet Wire, 44 AWG Enameled Copper - 5 Spool Sizes, 2020) [3], and 0.15 mm stainless steel hard rods (Stainless steel hard rods - 302 - 0.15 mm/0.0059 inch, 2019) [4]. The steel rods would be used as a structure for winding the coils. A complete device requires two coils (shown in Figure 1) including an excitation coil and a pick-up coil. Once the coils are wound, the steel rod would be removed and the core would be inserted in its place.

2. CONCLUSION

Of the approaches attempted in this study, approach #4 seems the most promising because it is the most practical for incorporating multi-layered coils, which is necessary for creating a complete magnetometer. The designs for the first three approaches that used aerosol jet printing only attempted single-layer coil devices and none of those were successful for creating a coil around the core material. Approach #4 shows the most promise because the winding process can be automated and the dimensions are on a similar scale as the aerosol jet printing. Compared to the printed wires, the solid wires also provide better conductivity and create a complete circuit more reliably.

Approach #4 seems promising to create smaller, more sensitive magnetometer sensors. In this study, only the coil was developed, without the rest of the supporting electronics for the complete magnetometer device. Future work would involve using approach #4 to create the excitation and pick-up coils. Then, the other electronics for data acquisition, processing, and storage will be incorporated, so the power consumption of the new magnetometer can be assessed.

This page is intentionally blank.

REFERENCES

1. Arias-Thode, Y., Hsu, L., Anderson, G., Babauta, J., Fransham, R., Obraztsova, A., . . . Chadwick, D. (2017). Demonstration of the SeptiStrand benthic microbial fuel cell powering a magnetometer for ship detection. Journal of Power Sources, 419-429. doi:10.1016/j.jpowsour.2017.03.045
2. Baranov, S. A., Larin, V. S., & Torcunov, A. V. (2017). Technology, Preparation and Properties of the Cast Glass-Coated Magnetic Microwires. Crystals. doi:10.3390/cryst7060136
3. Magnet Wire, 44 AWG Enameled Copper - 5 Spool Sizes. (2020). Retrieved from Remington Industries: https://www.remingtonindustries.com/magnet-wire/magnet-wire-44-awg-enameled-copper-5-spool-sizes/
4. Stainless steel hard rods - 302 - 0.15 mm/0.0059 inch. (2019). Retrieved from Stainless Steel Wire: https://stainless-wire.us/stainless-steel-rods/hard-rods/product/stainless-steel-hard-rods-15233.html
5. Trigona, C., Sinatra, V., Andò, B., Baglio, S., & Bulsara, A. R. (2017). Flexible Microwire Residence Times Difference Fluxgate Magnetometer. IEEE Transactions on Instrumentation and Measurement, 66(3), 559-568. doi:10.1109/tim.2016.2644918

This page is intentionally blank.

INITIAL DISTRIBUTION

84310	Technical Library/Archives	(1)
71780	K. Liotta	(1)
71780	E. Bozeman	(1)
81510	A. Sarmiento	(1)
71760	L. Hsu	(1)
71760	M. Arias-Thode	(1)

Defense Technical Information Center
Fort Belvoir, VA 22060–6218 (1)

NISE, Dr. Dave Rees (1)

The Office of Naval Research
Dr. Laura Kienker laura.kienker@navy.mil (1)

This page is intentionally blank.

REPORT DOCUMENTATION PAGE

Form Approved
OMB No. 0704-01-0188

PLEASE DO NOT RETURN YOUR FORM TO THE ABOVE ADDRESS.

1. REPORT DATE *(DD-MM-YYYY)*	2. REPORT TYPE	3. DATES COVERED *(From - To)*
September 2021	Final	

4. TITLE AND SUBTITLE

Method Development for Magnetometer Coils Using Additive Manufacturing

5a. CONTRACT NUMBER

5b. GRANT NUMBER

5c. PROGRAM ELEMENT NUMBER

6. AUTHORS

Kathryn Liotta
Eric Bozeman
NIWC Pacific

Angelica Sarmiento
Lewis Hsu
NIWC Pacific

Y. Meriah Arias-Thode
NIWC Pacific

5d. PROJECT NUMBER

5e. TASK NUMBER

5f. WORK UNIT NUMBER

7. PERFORMING ORGANIZATION NAME(S) AND ADDRESS(ES)

NIWC Pacific
53560 Hull Street
San Diego, CA 92152–5001

8. PERFORMING ORGANIZATION REPORT NUMBER

TD-3409

9. SPONSORING/MONITORING AGENCY NAME(S) AND ADDRESS(ES)

Dr. Linda Chrisey/Dr. Laura Kienker, Office of Naval Research, Code 342
875 N. Randolph Street
Arlington, VA 22203

10. SPONSOR/MONITOR'S ACRONYM(S)

NISE, ONR, NACC

11. SPONSOR/MONITOR'S REPORT NUMBER(S)

12. DISTRIBUTION/AVAILABILITY STATEMENT

DISTRIBUTION STATEMENT A: Approved for public release. Distribution is unlimited.

13. SUPPLEMENTARY NOTES

14. ABSTRACT

This report presents the methods and results of a short study with the goal of producing fluxgate magnetometer sensors with a higher sensitivity and lower power requirements than the first generation designed by the Non-Linear Dynamics group at Naval Information Warfare Center (NIWC) Pacific. To achieve this goal, additive manufacturing technology was evaluated as a means to increase sensitivity and decrease power requirements. The windings of the magnetometer sensor should have a smaller diameter and be closer to the core material to decrease the air gap to increase sensitivity in the pick-up coil, and reduce power requirements for the excitation coil. Most methods presented in this report focus on the use of the Optomec aerosol jet printer, and outlined are the challenges of each method. A more likely approach to solve these issues is also presented; and this is the use of actual wires for the windings instead of depending on the additive manufactured conductive lines.

15. SUBJECT TERMS

magnetometer; sensor; fluxgate; additive manufacturing; aerosol jet printing; ferromagnetic; low-power sensor

16. SECURITY CLASSIFICATION OF:			17. LIMITATION OF ABSTRACT	18. NUMBER OF PAGES	19a. NAME OF RESPONSIBLE PERSON
a. REPORT	b. ABSTRACT	c. THIS PAGE			Kathryn Liotta
U	U	U	SAR	32	19B. TELEPHONE NUMBER *(Include area code)* (619) 553-9771

This page is intentionally blank.

This page is intentionally blank.

Naval Information Warfare Center Pacific (NIWC Pacific)
San Diego, CA 92152-5001